

Final Report

Department of Energy, award/contract # DE-FG02-03ER15487

Title: Computational Nanophotonics: modeling optical interactions and transport in tailored nanosystem architectures

Principal Investigators: George C. Schatz, Mark A. Ratner

Abstract

This report describes research by George Schatz and Mark Ratner that was done over the period 10/03-5/09 at Northwestern University. This research project was part of a larger research project with the same title led by Stephen Gray at Argonne. A significant amount of our work involved collaborations with Gray, and there were many joint publications as summarized later. In addition, a lot of this work involved collaborations with experimental groups at Northwestern, Argonne, and elsewhere. The research was primarily concerned with developing theory and computational methods that can be used to describe the interaction of light with noble metal nanoparticles (especially silver) that are capable of plasmon excitation. Classical electrodynamics provides a powerful approach for performing these studies, so much of this research project involved the development of methods for solving Maxwell's equations, including both linear and nonlinear effects, and examining a wide range of nanostructures, including particles, particle arrays, metal films, films with holes, and combinations of metal nanostructures with polymers and other dielectrics. In addition, our work broke new ground in the development of quantum mechanical methods to describe plasmonic effects based on the use of time dependent density functional theory, and we developed new theory concerned with the coupling of plasmons to electrical transport in molecular wire structures. Applications of our technology were aimed at the development of plasmonic devices as components of optoelectronic circuits, plasmons for spectroscopy applications, and plasmons for energy-related applications.

Introduction

Surface plasmons (SPs) are collective excitations of the conduction electrons near the surfaces of metallic structures. The goal of this project was to develop theories, computational methods¹⁻³ and software that can be used to model the optical properties of these metallic nanostructures, and to adapt this software to describe experiments on structures ranging from a few nm to several μm in size.⁴⁻²⁷ With these tools and theories we have studied such processes as extinction, absorption and surface enhanced Raman spectroscopy (SERS) in nanoparticles and metal films,^{4, 15, 20} plasmon enhanced transmission and sensing with nanostructured metal films,^{6-9, 11-14} near-field imaging,^{5, 16-18, 25, 26} nonlinear effects such as the optical Kerr effect in conjunction with plasmon excitation,^{10, 27} photoemission from nanoparticles,¹⁹ plasmon enhanced dye sensitized solar cells,^{28, 29} and optical force experiments where near-fields are used to manipulate nanoparticles.²¹⁻²⁴ We have also developed the formalism and performed model studies concerned with the coupling of plasmon excitation to electron transport.³⁰⁻³² In addition, we have developed the formalism for combining time-dependent density functional theory (TDDFT) methods³³ for describing metal clusters as large as Ag_{120} ³⁴ with our continuum electrodynamics methods, making it possible deal with problems like molecules adsorbed on

particle surfaces where both short range (electronic structure) and long range (electrodynamics) play important roles.

Below is a brief description of projects completed under our DOE support. Publications resulting from the project are given in Refs. 1-34.

A. Codes and methods

Solving Maxwell's equations for complex metallic nanostructures is most conveniently done using numerical methods in which the metals and other system components (i.e., dielectrics) are represented using grids and/or discrete elements such as cubes or tetrahedra. There are numerous methods for doing this, and the methods we have found most useful have come in three flavors: the finite-difference time-domain (FDTD) method, the discrete dipole approximation (DDA) method, and the finite element method based on Whitney forms (FE-WF). These methods have been developed over the years, but in all cases we have added new content to these methods either in the form of new codes, new or improved algorithms, new simulation capabilities, or new properties. Here is a brief description of what we have done with each method:

A.1 Finite Difference Time Domain Method

The FDTD method represents the electric and magnetic fields on three-dimensional grids and propagates them in time according to Maxwell's equations. The book by Taflove and Hagness³⁵ documents the modern version of the method, which incorporates a variety of embellishments, such as special techniques for introducing incident waves and absorbing outgoing waves, that allow the method to simulate very complex structures. While some excellent commercial FDTD software packages exist, we have developed (in collaboration with Stephen Gray) in-house FDTD codes, some of which we routinely implement on massively parallel computer architectures. These codes implement our own models for describing realistically the metallic parts of the systems and allow us great flexibility for describing complex structures and nonlinear optical materials.

A.2 Discrete Dipole Approximation Method

The DDA method dates to Purcell and Pennypacker,³⁶ and was extensively developed by Draine and coworkers to applications to grains in the interstellar medium.³⁷ The DDA method assumes that the object of interest is represented by an array of cubic elements, each of which has a dipole polarizability that is determined³⁸ by the bulk dielectric function of the material associated with that cube. In the presence of an applied field, there is an induced polarization in each cube by this field, and by the induced dipoles in the other cubes. The cubes are assumed small enough that higher multipoles in each cube can be neglected. However fully retarded dipolar couplings between dipoles are included, so particles of any size can be described. Draine and coworkers have developed very efficient algorithms for determining the induced polarizations by solving the coupled dipole equations using complex conjugate gradient methods, and with the dipole coupling represented in Fourier space. Once the induced polarizations are determined, all far-field properties can be calculated. This method is not exact, but we have tested it for a wide variety of structures by comparing with FDTD or other exact results, and the results are generally in good agreement (few percent for extinction cross sections) provided that the dipole grid spacing is chosen small enough (values comparable to what are needed in FDTD are required).

Draine has developed a public-domain code that is available on his web site.³⁹ This code did not provide electromagnetic fields until the spring of 2008, and it still does not determine spectroscopic properties other than extinction, absorption and Rayleigh scattering, so we have extensively revised it in our work. We have also added the capabilities for describing a variety of complex nano-structures, for structures described with periodic boundary conditions, and for particles surrounded by solvent. We do not yet have a parallel version of the code, however Draine tells us that he is developing one, so we have decided not to pursue this until we see what Draine develops.

A.3 Whitney Form Finite Element Method

While conceptually simple, the finite element (FE) method,⁴⁰ particularly the full vectorial form often required for non-trivial plasmonics simulations, is the most technically challenging and sophisticated of the numerical approaches we have implemented. Our in-house full vectorial FE code is based on the use of Whitney Forms (WF) to describe the elements which allow correct (divergence free) electromagnetic field simulations. Because of the ability of the FE-WF approach to naturally adapt to the structures in question and satisfy exactly the correct boundary conditions, this approach is particularly useful for efficiently obtaining very accurate estimates of near-field intensities.³

B. Extinction, absorption and SERS in metal nanostructures

We completed several projects in which the electrodynamics codes described above were used to model light scattering from nanoparticles or other nanostructures, and the results were

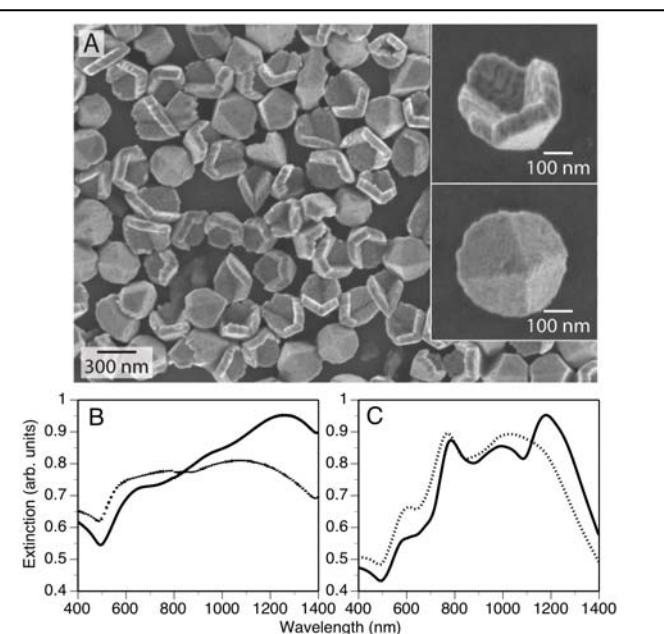


Figure 1. SEM images of the gold pyramidal shell particles, along with (B) experimental, and (C) calculated extinction spectra. Solid curves refer to spectra for the intact pyramids while dotted curves refer to pyramids in which the tips have been omitted in the fabrication.

used to interpret experimental studies of extinction or absorption spectra, or electromagnetic contributions to SERS. These results are very sensitive to the shape and size of the nanoparticle, and particularly for particles with complex structures, the interpretation of spectra in terms of polarization effects and multipole plasmon modes is difficult. Thus a computational electrodynamics study can often be of great use. In the work of Shuford et al.,¹⁵ we examined the scattering spectra of gold pyramidal-shape nanoparticles that are made using a soft-lithography method, and we demonstrated that in addition to the expected TE mode resonances, an unusual TM resonance also occurs that can be used as a switch due to sensitivity of this resonance intensity to small changes in particle structure.

Figure 1 presents pictures of the particles, along with a comparison of theory and

experiment for the extinction cross section. Both the experimental and theoretical results show that the plasmon resonance at about 1000 nm in the solid curve disappears in the dotted curve,

corresponding to a slight structural change in the particles in which the tips of the pyramids are omitted in their fabrication.

Other projects that were supported by the project involved the study of surface enhanced infrared absorption⁴ and of SERS.²⁰ Very recently we used our electrodynamics methods in a collaboration with Joe Hupp to describe the encapsulation of silver nanoparticles by TiO₂ for applications in dye-sensitized solar cells.^{29, 41} This work demonstrated that relatively thin films provide a pin-hole free coating for which there are enhanced electromagnetic fields outside the TiO₂ surface. This is important precursor work to the development of plasmon-enhanced solar cells.

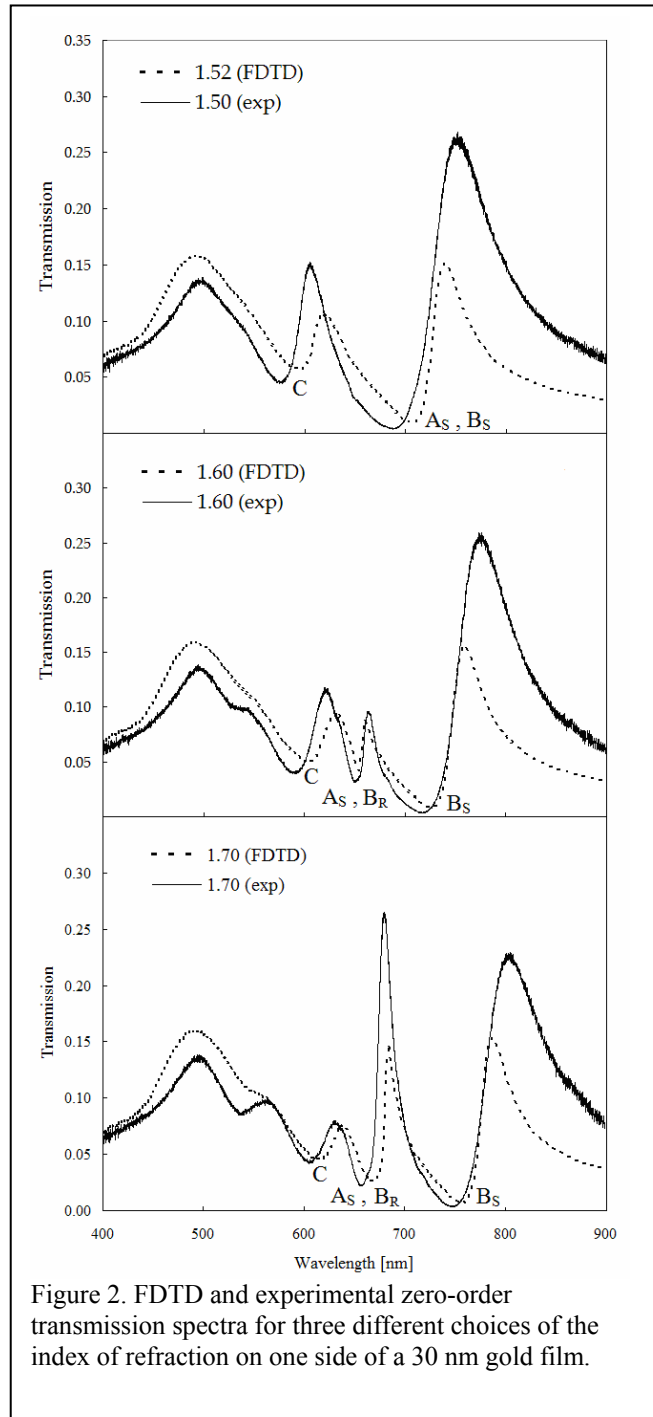


Figure 2. FDTD and experimental zero-order transmission spectra for three different choices of the index of refraction on one side of a 30 nm gold film.

C. Plasmon enhanced transmission in nanostructured films

A major direction for our work was to model experiments concerned with the transmission of light through thin gold films that contain either isolated holes or arrays of holes.^{6-9, 11-13} Thin gold films exhibit surface plasmon polariton (SPP) excitations, but they cannot be excited directly with light unless there is a mechanism for satisfying momentum conservation. Holes and hole arrays provide the necessary coupling, and this leads to a variety of possible excitations, including Bloch-wave SPPs, Rayleigh anomalies and localized SPs. Moreover, the wavelength of these excitations depends on local dielectric environment, which can be different on each side of the film, on the coupling between excitations on different sides of the film (depends on film thickness and wavelength), and on hole size, shape and spacing. In addition, the results vary with angle of incidence and with output scattering direction, and there are many possible directions for varying film composition, including multiple layers, and structures which combine holes with particles. Figure 2 shows an important result which came out of a collaboration with Teri Odom (Northwestern)¹² in which we discovered that it is possible to combine SPP excitation on one side of a gold film with Rayleigh Anomaly excitation on the other side. This RA-SPP coupling tunes

into resonance as the index of refraction on the SPP side is varied, leading to a sharp peak at 680 nm. (The other peaks in Fig. 2 do not depend on the simultaneous coupling of two different kinds of excitation.) The RA-SPP peak has very high sensitivity to the local index on the SPP side of the film, and because it is so narrow, it provides an excellent target for the development of chemical sensors that measure index of refraction changes. Noteworthy about this theory/experiment collaboration is that although unusual structure in the transmission spectra was initially discovered in the experiments, it was only as a result of the theoretical analysis that the origin of the effect was revealed, and subsequently the FDTD calculations were used to optimize the effect for choices of index of refraction that are of relevance to chemical sensing.

D. Near-field imaging

Our calculations can reveal the electromagnetic fields in the vicinity of metallic nanostructures, i.e., the evanescent near-fields which can be intense and localized owing to surface plasmon excitations. Experimental information about such fields is obtained using near-field scanning microscopes (NSOMs), which are probes that are brought close to the structures in question. A question that can arise is whether or not the NSOM itself is affecting the near-fields. We were able to address this question directly with full three-dimensional FDTD simulations that explicitly included the NSOM probe and a nanohole in a gold film.⁴² Interestingly, we found that the probe picks up information about electric field components parallel to the surface that match results that can be obtained in the absence of the probe. Our results were found to be in excellent accord with experimental observations.

In collaboration with Stephen Gray, other Argonne scientists and experimentalists from Troyes (France), we also explored a "non-invasive" procedure for imaging near-fields.^{5, 16} It turns out that polymers doped with certain azobenzene molecules can respond to the intense near-fields around nanoparticles. When a nanoparticle system is coated with a thin layer of such a polymer and exposed to light of an appropriate wavelength, the surface of the polymer distorts where the near-fields are high. After exposure, the near-field information is effectively frozen in the surface topography which can be measured with atomic force microscopy. Our detailed FDTD and DDA calculations of the near-fields were shown to correlate very well with a picture of rapid trans-cis-trans isomerizations of the azobenzene molecules that leads to molecular transport away from electromagnetic hot spots, i.e. our calculated field intensities were high where the surface topography exhibited a dip. Thus, roughly speaking, the surface topography represents a negative image of the near-field intensity.

We have also studied (in a collaboration with Teri Odom) near-field imaging associated with the optical corral structures such as gold rings.^{25, 26} Here we demonstrated that NSOM is sensitive to the electromagnetic mode structure that is set up by the corral close to the surface on which the corral is located. A simple electromagnetic model was defined where the corral is replaced by a perfect conductor, and it was found that this reproduces the mode structure, providing a simple (almost analytical) explanation for the observations.

E. Nonlinear effects

Nonlinear optical responses, e.g. second harmonic generation, arise from quadratic and higher order nonlinearities in the electric-field dependence of the polarization or induced dipole moment of a system. In collaboration with Stephen Gray we used the FDTD method to study the effect of an optical Kerr (third order) nonlinearity on a system of two metallic nanowires with an organic nonlinear polymer material between them.¹⁰ When the system is exposed to an ultrafast

pulse, the resulting transient near-field intensities showed remarkable dependence on the incident intensity. For low intensities ($< 1 \text{ MW/cm}^2$) the near-fields were most intense between the nanoparticles, a common result. However for intensities in the GW/cm^2 range, there is effectively no near-field intensity between the particles. We were able to partially understand this effect in terms of changes in the effective refractive index. The ability to control just where hot spots occur (or do not occur) by changing the incident intensity is an interesting phenomenon that could also have practical consequences for the development of nanophotonics-based switching devices. In related work we have recently discovered (in a collaboration with Chad Mirkin at Northwestern) a Kerr enhanced Raman effect that is driven by plasmon excitation.²⁷

F. photoelectron angular distributions

A collaboration with Steve Leone's group provided a new challenge for our electrodynamics calculations, which was to model the angular distribution of the emitted photoelectrons from NaCl nanoparticles having radii between 25 and 250 nm for photon energies in the 10-12 eV range. At these wavelengths, NaCl is a relatively strong absorber, but light can penetrate typically 15 nm into the particle. The resulting photoelectron can then escape from the particle, with a escape length which we estimate to be 10 nm. When these two processes are combined, using Mie theory (for assumed spherical particles) for photoexcitation at each point within the nanoparticle, and a dipole excitation model for the angular distribution of the emitted electron from each point, with exponential attenuation of the emitted electrons before they leave the particle, the resulting angular distribution varies from isotropic for small particles ($< 40 \text{ nm}$) to highly backward peaked for larger particles ($> 100 \text{ nm}$). Figure 3 shows the ratio of forward to backward scattering as a function of particle size, and we see that theory and experiment show similar behavior. Similar studies of gold nanoparticles showed only isotropic angular distributions in the 10-12 eV range of photon energies, due to the large escape depth of the few eV photoelectrons that are produced in the particle. Although this project did not involve conditions where plasmon excitation plays a role, this effect would automatically be included in the theory we developed when relevant. Of importance for the present proposal is that this model of photoionization/photoemission can be used as a basis for plasmon enhanced electron transfer processes.

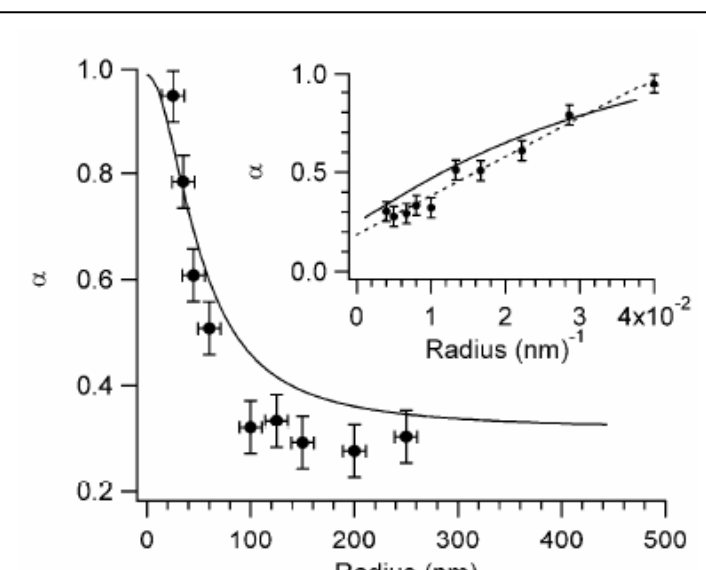


Figure 3. Ratio of forward to backward scattering of the emitted photoelectrons from NaCl at 10.9 eV, comparing theory and experiment.

that this model of photoionization/photoemission can be used as a basis for plasmon enhanced electron transfer processes.

G. Optical force effects

An electromagnetic field specified by \mathbf{E} and \mathbf{B} interacting with a particle exerts a time averaged force on that particle given by:

$$\langle F \rangle = \frac{1}{4} \operatorname{Re}(\alpha) \nabla |E|^2 + \frac{1}{2} k \operatorname{Im}(\alpha) \operatorname{Re}(E^* \times B) + \frac{1}{2} \operatorname{Im}(\alpha) \operatorname{Im}[(E^* \bullet \nabla) E]$$

where the complex polarizability α is assumed to be a scalar and $k=\omega/c$. Here the first term involves the gradient of the square of the electric field (a conservative force) while the second describes dissipation due to radiation pressure on the particle. The third term has only rarely been included, and even when it is left out, the explicit evaluation of $\langle F \rangle$ has only been done for spherical particles. In a series of projects²¹⁻²⁴ we developed ways to evaluate $\langle F \rangle$ for any particle shape based on discrete dipole approximation calculations (thereby solving Maxwell's equations for the particle), and we assessed the affect of the third term in the formula, with the goal of generating quantitative results for silver particles under circumstances where plasmon resonances could be excited.

The primary conclusions from this work are (1) that $\langle F \rangle$ is greatly enhanced when plasmon resonances play a role, and (2) the third term in the force equation often plays a significant role in the results under these circumstances. We also examined the interaction between two particles that results when they are close together, and a plane wave field interacts with them to produce strong plasmon excitation. We found that the interaction force can be strong enough to use this mechanism for particle trapping studies. However we found that the interaction of a molecule with a particle, or with two particles, is generally too weak to trap the molecule. This is an important conclusion for single molecule SERS experiments, where it has been postulated that such trapping events might be involved in blinking of the Raman signal.

H. Plasmon mediated electron transport

In a molecular transport junction, current passes through a single molecule under the influence of a voltage placed between two electrodes. The effect of photonic excitation on such junctions has been of interest experimentally^{43, 44}, and there are a few theoretical models in the literature.⁴⁵⁻⁴⁷ Plasmons represent a very special sort of excitation, however, one with much greater intensities, and substantially different physical form factors.

Understanding that one needs a more general approach than that in the literature (largely devoted to plane wave excitation), Ratner's group has worked in three areas: first, collaboration with Schatz and Gray has permitted deeper understanding of plasmonic excitations in metal arrays, particularly those with nanoholes.^{8, 9, 11} Second, independent work in Ratner's group was devoted to understanding optical forces between metallic particles in the presence of strong external fields.²¹⁻²⁴ Third, we have generalized the treatment of light excitation in molecular junctions, focusing on Raman spectra.^{31, 32}

The Raman model involves the usual non-equilibrium Green's function analysis for the transport, with a scattering theory approach to the optical excitations. Driving this to self-consistency, we are able to derive some important formal results: inverse Raman (initiated in the excited state that is generated by the non-linear voltage) can be observed, Raman spectra can report on the temperature of the molecule in the transport junction).^{31, 32}

Finally, we have worked to develop a state, rather than level, implementation of non-equilibrium Green's functions.³⁰ This has tremendous advantages: it is not limited to low voltages, because it can deal with the different isolated molecular states. It also may prove possible to solve the electronic structure of the molecule in the junction at a higher (correlated electron) level than is normally used in the density functional techniques that dominate the field at present. This approach has precursors in the literature, but we feel that it will be a productive

way to deal with correlation, and to fix some of the striking disagreements between transport theory and experiment that still exist in the literature.

Bibliography

1. McMahon, J. M.; Gray, S. K.; Schatz, G. C., A discrete action principle for electrodynamics and the construction of explicit symplectic integrators. *J. Comp. Phys.* **2009**, 228, 3421-3423.
2. Masiello, D. J.; Schatz, G. C., Many-body theory of surface-enhanced Raman scattering. *Phys. Rev. A* **2008**, 78, 042505/1-042505/24.
3. Zhao, J.; Pinchuk, A. O.; McMahon, J. M.; Li, S.; Ausman, L. K.; Atkinson, A. L.; Schatz, G. C., Methods for describing the electromagnetic properties of anisotropic silver and gold nanoparticles. *Accts. Chem. Res.* **2008**, 41, 1710-1720.
4. Chang, S.-H.; Schatz, G. C.; Gray, S. K., FDTD/TDSE study on surface-enhanced infrared absorption by metal nanoparticles. *Proc. SPIE-Int. Soc. Opt. Eng.* **2006**, 6323, (Plasmonics: Metallic Nanostructures and Their Optical Properties IV), 632321/1-632321/8.
5. Hubert, C.; Rumyantseva, A.; Lerondel, G.; Grand, J.; Kostcheev, S.; Billot, L.; Vial, A.; Bachelot, R.; Royer, P.; Chang, S.-h.; Gray, S. K.; Wiederrecht, G. P.; Schatz, G. C., Near-Field Photochemical Imaging of Noble Metal Nanostructures. *Nano Lett.* **2005**, 5, (4), 615-619.
6. Chang, S.-H.; Gray, S. K.; Schatz, G. C., Surface plasmon generation and light transmission by isolated nanoholes and arrays of nanoholes in thin metal films. *Opt. Express* **2005**, 13, 3150-65.
7. Kwak, E.-S.; Henzie, J.; Chang, S.-H.; Gray, S. K.; Schatz, G. C.; Odom, T. W., Surface Plasmon Standing Waves in Large-Area Subwavelength Hole Arrays. *Nano Lett.* **2005**, 5, (10), 1963-1967.
8. Shuford, K. L.; Ratner, M. A.; Gray, S. K.; Schatz, G. C., Finite-difference time-domain studies of light transmission through nanohole structures. *Appl. Phys. B* **2006**, 84, (1-2), 11-18.
9. Shuford, K. L.; Ratner, M. A.; Gray, S. K.; Schatz, G. C., Electric field enhancement and light transmission in cylindrical nanoholes. *J. Comput. Theor. Nanosci.* **2007**, 4, (2), 239-246.
10. Wang, X.; Schatz, G. C.; Gray, S. K., Ultrafast pulse excitation of a metallic nanosystem containing a Kerr nonlinear material. *Phys. Rev. B* **2006**, 74, (19), 195439/1-195439/5.
11. Shuford, K. L.; Gray, S. K.; Ratner, M. A.; Schatz, G. C., Substrate effects on surface plasmons in single nanoholes. *Chem. Phys. Lett.* **2007**, 435, (1-3), 123-126.
12. McMahon, J. M.; Henzie, J.; Odom, T. W.; Schatz, G. C.; Gray, S. K., Tailoring the sensing capabilities of nanohole arrays in gold films with Rayleigh anomaly-surface plasmon polaritons. *Opt. Express* **2007**, 15, 18119-29.
13. Schatz, G. C.; McMahon, J. M.; Gray, S. K., Tailoring the parameters of nanohole arrays in gold films for sensing applications. *Proc. SPIE-Int. Soc. Opt. Eng.* **2007**, 6641, (Plasmonics: Metallic Nanostructures and Their Optical Properties V), 664103/1-664103/8.
14. Gray, S. K.; Lee, T.-W.; Chang, S.-H.; Schatz, G. C., Electrodynamics simulations of surface plasmon behavior in metallic nanostructures. *Proc. SPIE-Int. Soc. Opt. Eng.* **2005**, 5927, (Plasmonics: Metallic Nanostructures and Their Optical Properties III), 59270H/1-59270H/6.
15. Shuford, K. L.; Lee, J.; Odom, T. W.; Schatz, G. C., Optical properties of gold pyramidal shape nanoshells. *J. Phys. Chem. C* **2008**, 112, 6662-6.

16. Hubert, C.; Bachelot, R.; Plain, J.; Kostechhv, S.; Lerondel, G.; Mathieu, J.; Royer, P.; Zou, S.; Schatz, G. C.; Wiederrecht, G.; Gray, S. K., Near-field polarization effects in molecular-motion-induced photochemical imaging. *J. Phys. Chem. C* **2008**, 112, 4111-6.

17. Boneberg, J.; Koenig-Birk, J.; Muenzer, H. J.; Leiderer, P.; Shuford, K. L.; Schatz, G. C., Optical near-fields of triangular nanostructures. *Appl. Phys. A* **2007**, 89, (2), 299-303.

18. Achermann, M.; Shuford, K. L.; Schatz, G. C.; Dahanayaka, D. H.; Bumm, L. A.; Klimov, V. I., Near-field spectroscopy of surface plasmons in flat gold nanoparticles. *Opt. Lett.* **2007**, 32, (15), 2254-2256.

19. Wilson, K. R.; Zou, S.; Shu, J.; Ruehl, E.; Leone, S. R.; Schatz, G. C.; Ahmed, M., Size-Dependent Angular Distributions of Low-Energy Photoelectrons Emitted from NaCl Nanoparticles. *Nano Lett.* **2007**, 7, (7), 2014-2019.

20. Reilly, T. H., III; Chang, S.-H.; Corbman, J. D.; Schatz, G. C.; Rowlen, K. L., Quantitative Evaluation of Plasmon Enhanced Raman Scattering from Nanoaperture Arrays. *J. Phys. Chem. C* **2007**, 111, (4), 1689-1694.

21. Wong, V.; Ratner, M. A., Size dependence of gradient and nongradient optical forces in silver nanoparticles. *J. Opt. Soc. Am. B* **2007**, 24, (1), 106-112.

22. Wong, V.; Ratner, M. A., Gradient and nongradient contributions to plasmon-enhanced optical forces on silver nanoparticles. *Phys. Rev. B* **2006**, 73, (7), 075416/1-075416/6.

23. Wong, V.; Ratner, M. A., Explicit computation of gradient and nongradient contributions to optical forces in the discrete-dipole approximation. *J. Opt. Soc. Am. B* **2006**, 23, (9), 1801-1814.

24. Wong, V.; Ratner, M. A., Geometry Dependent Features of Optically Induced Forces between Silver Nanoparticles. *J. Phys. Chem. B* **2006**, 110, (39), 19243-19253.

25. Babayan, Y.; McMahon, J. M.; Li, S.; Gray, S. K.; Schatz, G. C.; Odom, T. W., Confining standing waves in optical corrals. *ACS Nano* **2009**, 3, 615-620.

26. McMahon, J. M.; Gray, S. K.; Schatz, G. C., Dephasing of electromagnetic fields in scattering from an isolated slit in a gold film. In *Plasmonics: Nanoimaging, Nanofabrication, and Their Applications IV, SPIE Proceedings*, Kawata, S.; Shalaev, V. M.; Tsai, D. P., Eds. 2008; Vol. 7033, pp 1-6.

27. Wei, W.; Li, S.; Qin, L.; Xue, C.; Millstone, J. E.; Xu, X.; Schatz, G. C.; Mirkin, C. A., Surface plasmon-mediated energy transfer in hetero-gap Au-Ag Nanowires. *Nano Lett.* **2008**, 8, 3446-9.

28. Standridge, S. D.; Schatz, G. C.; Hupp, J. T., Distance Dependence of Plasmon-Enhanced Photocurrent in Dye-Sensitized Solar Cells. *J. Amer. Chem. Soc.* **2009**, ACS ASAP.

29. Standridge, G. C.; Schatz, G. C.; Hupp, J. T., Protection of silver nanoparticles using atomic layer deposition of TiO₂. *Langmuir* **2008**, 25, 2596-2600.

30. Galperin, M.; Nitzan, A.; Ratner, M., Inelastic transport in the Coulomb blockade regime within a nonequilibrium atomic limit. *Phys. Rev. B* **2008**, 78, 125320/1-125320/9.

31. Galperin, M.; Nitzan, A.; Ratner, M., Raman Scattering in Current Carrying Molecular Junctions. *J. Chem. Phys.* **2009**, 130, 144109/1-144109/19.

32. Galperin, M.; Ratner, M.; Nitzan, A., Raman scattering from nonequilibrium molecular conduction junctions. *Nano Lett.* **2009**, 9, 758-762.

33. Jensen, L.; Aikens, C. M.; Schatz, G. C., Electronic structure methods for studying surface-enhanced Raman scattering. *Chem. Soc. Rev.* **2008**, 37, 1061-73.

34. Aikens, C. M.; Li, S.; Schatz, G. C., From discrete electronic states to plasmons: TDDFT optical absorption properties of Agn(n=10,20,35,56,84,120) tetrahedral clusters. *J. Phys. Chem. C* **2008**, 112, 11272-11279.

35. Hagness, S. C.; Taflove, A., *Computational Electrodynamics: The Finite-Difference Time-Domain Method*. 3rd ed.; Artech House: Boston, 2005.

36. Purcell, E. M.; Pennypacker, C. R., Scattering and absorption of light by nonspherical grains. *Astrophys. J.* **1973**, 186, 705-714.

37. Draine, B. T.; Flatau, P. J., Discrete-dipole approximation for scattering calculations. *J. Opt. Soc. Amer. A* **1994**, 11, (1491-1499).

38. Draine, B. T.; Goodman, J., Beyond Clausius-Mossotti: wave propagation on a polarizable point lattice and the discrete dipole approximation. *Astrophys. J.* **1993**, 405, 685-697.

39. Draine, B. T.; Flatau, P. J., "User guide to the Discrete Dipole Approximation Code DDSCAT 6.1" <http://arxiv.org/abs/astro-ph/0409262v2>. 2004.

40. Jin, J., *The Finite Element Method in Electrodynamics*. 2nd ed.; Wiley: New York, 2002.

41. Standridge, S. D.; Schatz, G. C.; Hupp, J. T., Distance Dependence of Plasmon-Enhanced Photocurrent in Dye-Sensitized Solar Cells. *J. Amer. Chem. Soc., ACS ASAP*.

42. Yin, L.; Vlasko-Vlasov, V. K.; Rydh, A.; Pearson, J.; Welp, U.; Chang, S. H.; Gray, S. K.; Schatz, G. C.; Brown, D. B.; Kimball, C. W., Surface plasmons at single nanoholes in Au films. *Appl. Phys. Lett.* **2004**, 85, (3), 467-469.

43. Wu, S.; Ogawa, N.; Ho, W., Atomic-Scale Coupling of Photons to Single-Molecule Junctions. *Science* **2006**, 312, 1362-5.

44. Diesling, D.; Merschdorf, M.; A., T.; Pfeiffer, W., Identification of Multiphoton-induced Photocurrents in Metal-Insulator-Metal Junctions. *Appl. Phys. B* **2004**, 78, 443-6.

45. Tikhonov, A.; Coalson, R. D.; Dahnovsky, Y., Calculating electron current in a tight-binding model of a field-driven molecular wire: Application to xylyl-dithiol. *J. Chem. Phys.* **2002**, 117, (2), 567-580.

46. Lehmann, J.; Kohler, S.; Hanggi, P.; Nitzan, A., Rectification of laser-induced electronic transport through molecules. *J. Chem. Phys.* **2003**, 118, (7), 3283-3293.

47. Urdaneta, I.; Keller, A.; Atabek, O.; Mujica, V., Laser-induced nonlinear response in photoassisted resonant electronic transport. *J. Chem. Phys.* **2007**, 127, (15), 154110/1-154110/9.